Competing structural phase sequences in $(C_3H_7NH_3)_2CuCl_4$: reconstructive phase transitions and the low-temperature incommensurate phase

1994 J. Phys.: Condens. Matter 6 10839

(http://iopscience.iop.org/0953-8984/6/49/024)

J. Phys.: Condens. Matter 6 (1994) 10839–10853. Printed in the UK

Competing structural phase sequences in $(C_3H_7NH_3)_2CuCl_4$: reconstructive phase transitions and the low-temperature incommensurate phase†

I R Jahn, K Schwab, K Knorr and K Holocher

Institut für Kristallographie der Universität Tübingen, Charlottenstrasse 33, D-72070 Tübingen, Germany

Received 22 June 1994, in final form 26 August 1994

Abstract. The structural phase sequence of $(C_3H_7NH_3)_2CuCl_4$ (abbreviated to C_3CuCl) has been determined between 20 and 300 K by optical and x-ray methods. The Jahn–Teller compound undergoes two types of reconstructive phase transition between antiferrodistortive (AF) and ferrodistortive (F) structures: the first may be characterized by a spontaneous 90° switching of the long Jahn–Teller axes of the octahedra within every second layer ('octahedron-axes switching' (OAS)), and the second by a spontaneous reorientation of the hydrogen-bonding pattern ('hydrogen-bond switching' (HBS)) in the whole crystal. With these mechanisms, the highly unusual sequence of the phases $\delta(Pbca, Z = 4)$, $\varepsilon(P2_1/n11, Z = 2)$, $\zeta(\text{IC}(P2_1/n11))$, and $\eta(P2_1/c11, Z = 4)$ is

$$\delta - 180\ \text{K}(\text{OAS}) \rightarrow \zeta - 132\ \text{K}(\text{HBS}) \rightarrow \eta, \delta \leftarrow 192\ \text{K}(\text{OAS}) - \varepsilon \leftarrow 180\ \text{K} - \zeta \leftarrow 141\ \text{K}(\text{HBS}) - \eta.$$

On cooling, the OAS transition at 180 K leads directly to the incommensurate (IC) ζ phase with a modulation wavevector $q_\zeta = 0.58t_2^* + 0.08t_3^*$. On heating, the modulation disappears at the same temperature and, as a new phase, the symmetrical ε phase occurs; at 192 K, the compound switches back to the room-temperature δ phase. The structure of the low-temperature η phase, generated by the HBS mechanism, may be considered a distorted version of the twin structure of the δ phase. No symmetry relation exists between the IC ζ phase and the δ and η phases. We find that the complex transition sequence of C_3CuCl is in fact the result of two interfering phase sequences, namely those of the AF and F states, respectively. X-ray data on the high-temperature IC γ phase are also presented.

1. Introduction

The perovskite-type layer structures with the general formula $(C_nH_{2n+1}NH_3)_2MX_4$ ($M \equiv Mn^{2+}$, Fe^{2+}, Cu^{2+} or Cd^{2+}; $X \equiv Cl^-$ or Br^-; $n = 1, 2, 3, \ldots$), which is abbreviated hereafter to C_nMX, are known to exhibit a large variety of structural modifications (see, e.g., Kind (1980)). Recently, the propyl-ammonium ($n = 3$) compounds have attracted much interest because of their unusual transitions between commensurate (C) and incommensurate (IC) phases. The manganese compound C_3MnCl showing two IC phases has been studied in detail (see, e.g., Muralt *et al* (1982), Depmeier (1983), Depmeier and Mason (1983), Muralt (1986) and Muralt *et al* (1988)). In the high-temperature IC γ phase, the amplitude of the modulation wave with wavevector $0.18a^* + c^*$ vanishes on lowering the temperature, and

† Dedicated to Professor W Prandl on the occasion of his 60th birthday.

0953-8984/94/4910839+15$19.50

the high symmetry of the C β phase re-enters in the δ phase; at the low-temperature IC–C transition between the ε and ζ phases the modulation wavevector switches from $0.37b^*$ to $(b^* - c^*)/3$. In contrast, the isostructural C_3CdCl realizes only the low-temperature IC phase; at the lock-in transition the modulation wavelength jumps from $0.42b^*$ to b^* (Doudin and Chapuis 1988). In the copper compound C_3CuCl, so far only the high-temperature part of the phase sequence has been determined (Jahn *et al* 1989, Doudin and Chapuis 1990a, b):

$$\delta(Pbca) \leftarrow 383\ \text{K} \rightarrow \gamma(\text{IC}(Pbca)) \leftarrow 413\ \text{K} \rightarrow \beta(Pbca) \leftarrow 436\ \text{K} \rightarrow \alpha(Bbcm).$$

Although the structure is modified by the Jahn–Teller (JT) effect, the sequence with incommensurability and re-entrant behaviour is very similar to that of C_3MnCl.

In these structures, the layers consist of corner-sharing MCl_6 octahedra sandwiched between $C_nH_{2n+1}NH_3$ chains. The NH_3 heads of the chains occupy the cavities between neighbouring octahedra; one hydrogen bond is directed to an in-plane chlorine site and two bonds run to out-of-plane chlorine sites. Successive layers are staggered; they are coupled by van der Waals forces acting between the terminal methyl groups of the chains. For $n \leqslant 3$, the chains can be looked upon as rigid molecules. In the high-temperature α phase, the hydrogen-bonding system and chains are dynamically disordered. With the exception of the copper compounds, the structure of α is tetragonal (space group, $I4/mmm$). On cooling, the molecular motion freezes gradually. A great number of structural degrees of freedom on the one hand and the interplay of various weak interactions on the other hand cause complex phase sequences.

The copper compounds are very special. Owing to the JT distortion of the $CuCl_6$ octahedra the fourfold symmetry of the M site is lost in the disordered phase; the structure of α is orthorhombic with space group $Bbcm$. However, the interaction between adjacent layers is too weak to suppress the local fourfold symmetry at the NH_3 site. This is evidenced by the zero in-plane birefringence of the copper compounds in the α phase (Jahn *et al* 1989) as well as by the structure determination of C_3CuCl by Doudin and Chapuis (1990a). Consequently, the chain ordering within the orthorhombic matrix results in two structures: a ferrodistortive (F) monoclinic configuration with space group $P2_1/n(\equiv P12_1/n1$; equivalent to $P2_1/a$, $P2_1/c)$ realized in C_1CuCl (Papst *et al* 1987) and an antiferrodistortive (AF) orthorhombic configuration with $Pbca$ in the β and δ phases of C_3CuCl (Doudin and Chapuis 1990a). The symmetry groups of these phases are subgroups of $Bbcm$; the corresponding phase transitions occur at the Brillouin zone points Γ and Y, respectively. A very special situation arises in C_2CuCl; its sequence $Pbca \leftarrow 338$ K; 356 K $\rightarrow P2_1/n \leftarrow 364$ K $\rightarrow Bbcm$ indicates a spontaneous switching between the two configurations (Jahn *et al* 1989). This spectacular reconstructive transition between phases which are not symmetry related shows a large thermal hysteresis and is extremely sensitive to strains.

The aim of the present work is to explore the influence of the JT distortion on the low-temperature phases of C_3CuCl. We pay attention to the possible predispositions of this compound to a further IC phase and to a reconstructive phase transition. Preliminary birefringence and x-ray measurements (Jahn *et al* 1986) indicated reversible transitions around 135 K and at 180 K; however, a phase change at 192 K observed only on heating pointed to an intermediate phase which is omitted on cooling. Later results of birefringence, specific heat and thermal expansion measurements by Etxebarria *et al* (1988) gave no hint of an additional phase. It should be noted that our experiments have been extended to the mixed system $(C_3H_7NH_3)_2(Br_xCl_{1-x})_4$; a short account has been given by Schwab *et al* (1992).

Our paper is organized as follows. In section 2, the experimental methods used in this study will be described. Our earlier results on the high-temperature IC γ phase (Jahn *et al*

1989) had been given without experimental details; these will be described in section 3.1. The switching mechanisms active at the reconstructive phase transitions $\delta \rightarrow \zeta$, $\varepsilon \rightarrow \delta$ and $\zeta \rightarrow \eta$ are identified in sections 3.2 and 3.4, respectively. In section 3.3, the modulation wavevector of the IC ζ phase will be determined. The low-temperature phase sequence is discussed in section 4.

2. Experiments

Single crystals of C_3CuCl were grown at 40 °C by slow evaporation of a saturated aqueous solution containing stoichiometric amounts of $C_3H_7NH_3Cl$ and $CuCl_2$ (Arend *et al* 1978). For the measurements, as-grown crystal platelets were selected, untwinned and free from mechanical deformations and liquid inclusions. Birefringence and domain formation were studied under the polarizing microscope using N_2 cooling or an electrical heating stage. The relative retardations were compensated with an Ehringhaus rotary compensator.

Precession photographs were taken with graphite-monochromated molybdenum radiation. Temperatures down to 100 K could be obtained by blowing the sample with cold N_2 gas. Thereby the sample plate was water protected and fixed stress free between Kapton foils. The temperature could be stabilized to within 5 K.

The main part of the measurements was performed using a focusing single-crystal camera (Dachs and Knorr 1972) together with Cu $K\alpha_1$ radiation. The advantages of this camera are sharp reflection lines at a low background and a very short exposure time. For the temperature range between about 100 and 650 K, cooling and heating devices are available; a temperature controller allows measurements at constant T or any T scans linear in time. We used a special N_2 bath cryostat designed for top loading. Its small liquid reservoir is refilled continuously out of a second larger reservoir above the cryostat by means of two vacuum-insulated transfer lines; the permanent circulation of the cooling liquid is maintained by the lifting forces of the N_2 bubbles created by the heater close to the sample. The sample (2 mm × 2 mm × 0.2 mm) was kept between Kapton foils which were covered with silicon grease and mounted on a holder equipped with an adjusting device. A suitable orientation of the crystal had to be chosen outside the cryostat. Diffraction patterns were recorded by means of a film-lift set-up; during continuous heating or cooling the sample, the film is moved vertically, and exposures are made through a slit which lies in the horizontal scattering plane. The width of the slit (2 mm) together with the recorded temperature interval determine the accuracy of the temperature of an event recorded on the film. For a 50 K interval the uncertainty amounts to ±1 K.

Working in forward-reflection geometry we used oscillation angles in the range $10° < \theta < 40°$. The crystal plates limited the accessible part of the reciprocal lattice. Choosing the usual setting of the room-temperature δ phase with $a, b (a \simeq 7.6$ Å $> b \simeq 7.3$ Å) parallel to the layer plane and $c (c \simeq 24.6$ Å) perpendicular to it, the reciprocal planes $h0l$, $h1l$ and $0kl$, $1kl$ could be recorded. For the quantitative analysis the $0kl$ reflections were used. Intensity profiles corresponding to different sample temperatures were evaluated from the film by the use of a microdensitometer. In the case of very weak reflections the line positions were determined under the stereomicroscope with a glass rule as reference.

Powder diffraction patterns were recorded with a Guinier camera over the temperature range 300–20 K (Ihringer 1982). Line positions were determined by least-squares refinement of Gaussian profiles fitted to intensity data digitized with a microdensitometer. The lattice parameters at each temperature are obtained from the line positions by a least-squares fit again. It turned out that the process of powdering the soft C_3CuCl single crystals produced

highly strained grains with the consequence that the strongly discontinuous transition at around 135 K was partly suppressed. Satellite intensities were too weak to be detected on the powder pattern.

3. Structural phase sequence

A rapid survey of the phase transitions of C_3CuCl is given by the temperature-dependent linear birefringence of an as-grown (001) plate, $\Delta n = n_a - n_b$, shown in figure 1. In the copper compounds, anomalous dispersion disturbs the absolute compensation usually made with white light. Therefore, the Δn scale was based on the room-temperature refractive indices determined by Kusto (1988). Seven phases have been identified between 450 and 20 K. In table 1, they are listed with their ranges of stabilities, space groups, basic translations of the primitive cell and numbers of formula units. The data for the low temperature ε, ζ and η phases are the results of the present paper.

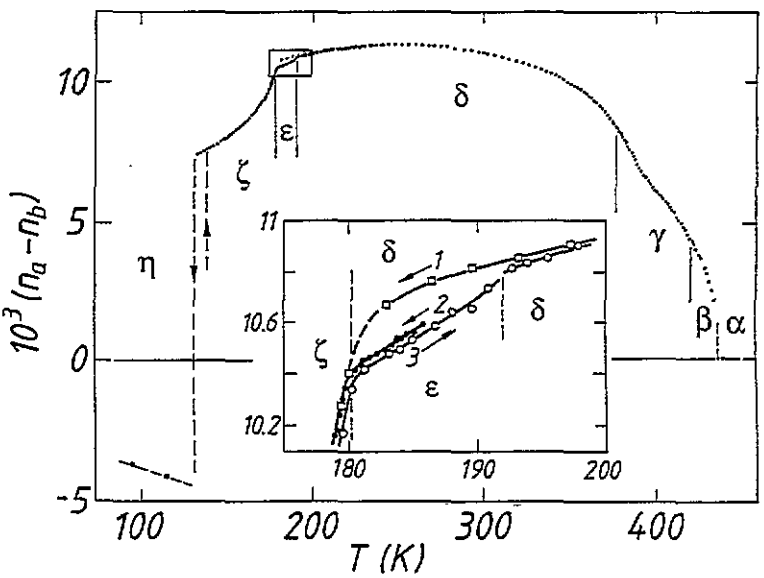

Figure 1. Linear birefringence of C_3CuCl versus temperature ($\lambda = 633$ nm).

3.1. The high-temperature incommensurate γ phase

The IC γ phase is characterized by a displacive modulation of the layers with the wavevector $q_\gamma = \kappa a^*$, $\kappa \simeq 0.18$ and a displacement vector parallel c (Doudin and Chapuis 1990b). In previous studies, the transition temperatures between the γ phase and the neighbouring β and δ phases have been determined either from the anomalous birefringence behaviour or the temperature-dependent x-ray scattering intensity of satellite reflections. Unfortunately, the optical results $T_{\beta\gamma} = 423$ K and $T_{\gamma\delta} = 378$ K obtained by Etxebarria *et al* (1988) and $T_{\beta\gamma} = 408$ K and $T_{\gamma\delta} = 379$ K obtained by Kusto (1988) differ as strongly as do the x-ray data of 413 K and 383 K obtained by Jahn *et al* (1989) and about 423 K and about

Table 1. The phase sequence of $(C_3H_7NH_3)_2CuCl_4$. The number Z of formula units is given for the primitive unit cell. The modulation wavevectors are defined with respect to the unit cell of the average structure (space group in parentheses), respectively. The basic vectors of the reciprocal lattice of the ε phase are $t_1^* = a^*$, $t_2^* = b^* + c^*$, $t_3^* = -b^* + c^*$. In the δ phase, $a \simeq 7.7$ Å, $b \simeq 7.3$ Å and $c \simeq 24.6$ Å. The arrows at the transition temperatures indicate which phase is attained on cooling or heating, respectively.

	$P2_1/c11$		$P2_1/n11$	$Pbca$		$Pbca$	$Bbcm$
	$Z = 4$	IC($P2_1/n11$)	$Z = 2$	$Z = 4$	IC ($Pbca$)	$Z = 4$	$Z = 2$
	a^*, b^*, c^*	$0.58t_2^* + 0.08t_3^*$	t_1^*, t_2^*, t_3^*	a^*, b^*, c^*	$0.18a^*$	a^*, b^*, c^*	$a^* + c^*, b^*, -a^* + c^*$
	η	ζ	ε	δ	γ	β	α
T (K)	←132—	←———180———→			383	413	436
	—141→	←180→	——192→				

378 K obtained by Doudin and Chapuis (1990b). The optical discrepancies can be easily explained from figure 1. Since the birefringence changes smoothly at the transition points, the extraction of $T_{\beta\gamma}$ and $T_{\gamma\delta}$ without any additional criterion must be rather arbitrary. The differing x-ray results, on the other hand, may arise because the satellite peaks are superimposed onto diffuse streaks which connect the satellite and reciprocal-lattice point. The temperature dependences of the streak and satellite intensity seem to be different.

We have studied the $2 \pm \kappa\, 0\, 1$ satellite reflections since they are easily accessible with our focusing single-crystal camera using as-grown (001) platelets as samples. The disadvantage of their weak intensity is compensated by the high resolution of the apparatus. Figure 2 shows temperature-dependent line profiles of the satellite $2 - \kappa\, 0\, 1$ obtained on a heating run. The integral intensity and half-width of the lines are presented in figures 3(*a*) and 3(*b*), respectively. The intensity decreases sharply at around 383 and 413 K, and at these temperatures the diffuse streaks begin to contribute as indicated by the increasing half-width. As known from experimental and theoretical work on C_3MnCl (Muralt 1986, Saito and Kobayashi 1992), the modulation amplitude drops steeply to zero at the boundaries of the γ phase. We therefore localize $T_{\beta\gamma}$ and $T_{\gamma\delta}$ at the temperatures given above. The satellite intensities measured by Doudin and Chapuis (1990b) exhibit strong tails down to 370 K and up to 430 K. In our experiment the diffuse part was weak; it could be followed up to about 420 K. The satellite half-width decreases with increasing temperature and/or with the length of the experimental time. Such behaviour might be caused by annealing defects.

The temperature dependence of the modulation component κ, given in figure 3(*c*), was calculated on the basis of the line positions of the $2 \pm \kappa\, 0\, 1$ satellites and the main reflection 200. The value obtained increases linearly with increasing temperature; the slope of 5×10^{-5} K^{-1} agrees quite well with the value of about 7×10^{-5} K^{-1} found for C_3MnCl (Depmeier 1983). This non-critical temperature dependence has been postulated theoretically by Muralt *et al* (1982). Our κ is slightly above the value 0.175(5) given by Doudin and Chapuis (1990b) for 400 K; interestingly, their value reproduces Depmeier's result on C_3MnCl. We should mention that second-order satellites appeared on overexposed precession photographs. The ratio of the integral intensities of the second- to the first-order satellites $12 - 2\kappa\, 0\, 0$ and $11 - \kappa\, 0\, 0$ amounts to about 1:60.

3.2. *Reconstructive $\delta \rightarrow \zeta$ and $\varepsilon \rightarrow \delta$ phase transitions*

In C_3MnCl the transition between the room-temperature δ phase and the low-temperature IC ε phase occurs at 163 K; the birefringence curve changes slope at this point (Brunskill

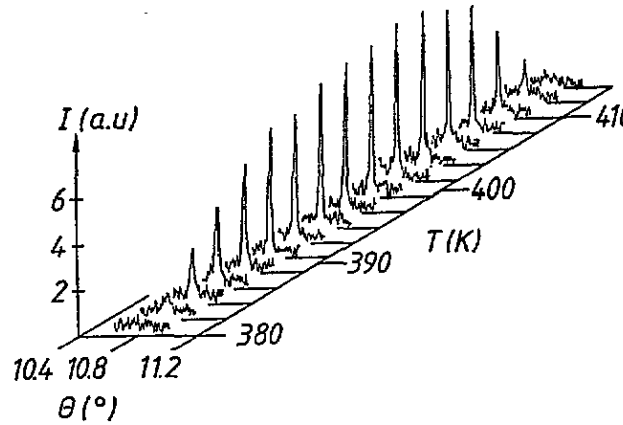

Figure 2. Line profile of the satellite reflection $2-\kappa\,0\,1$ of the γ phase as a function of temperature.

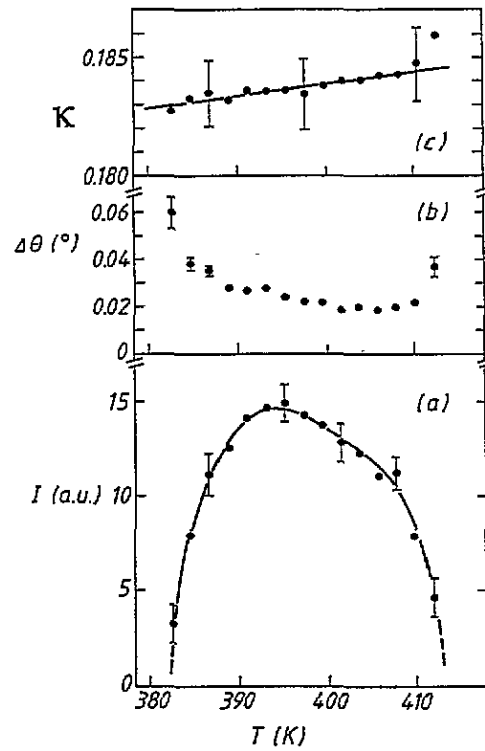

Figure 3. (*a*) Temperature-dependent integral intensity of the satellite reflection $2-\kappa\,0,1$ (a.u., arbitrary units), (*b*) its half-width and (*c*) the modulation vector component κ.

and Depmeier 1982). In C_3CuCl, the situation is more complex, as shown in the inset of figure 1. Cooling run 1 indicates a phase transition at around 180 K. The second cooling run after the sample had been heated to 186 K follows a new line above the transition

point. Curve 3 obtained on heating reproduces curve 2 and above 192 K coincides with the original curve 1. The small shift between cooling and heating curves, for curves 1 and 3 visible below 180 and above 192 K, is caused by a temperature lag between the sample and sensor in the cooling–heating device. At first, the birefringence 'loop' between 180 and 192 K looks like a hysteresis phenomenon at a strongly discontinuous phase transition. The data obtained by Etxebarria *et al* (1988) on birefringence, thermal expansion and specific heat cannot contribute much to this point; they were obtained either on cooling or heating only.

Our x-ray diffraction results disclose an exciting situation. In figure 4, small segments of the intensity profiles obtained over the range 155–205 K are represented. On cooling (figure 4(a)), the 024 line of the orthorhombic δ phase splits close to 180 K. Simultaneously, several new peaks with a very low intensity occur. In section 3.3, they will be identified as satellite reflections of an incommensurately modulated ζ phase. On heating (figure 4(b)), however, only the satellites disappear around 180 K; the main reflections retain their splitting, slightly reduced, up to 192 K. The identical main reflections below and above 180 K led us to conclude that the new ε phase between 180 and 192 K on heating is the symmetrical C phase of the IC ζ phase. The strongly discontinuous $\delta \longrightarrow \zeta$ and $\varepsilon \longrightarrow \delta$ phase transitions should be related to the same lattice instability. In strained crystals and in samples which have been cycled, the $\varepsilon \rightarrow \delta$ transition is spread to higher temperatures; the $\delta \rightarrow \zeta$ transition remains sharp.

To deduce the space group of the ε phase (and the average space group of ζ), the $h0l$, $h1l$, $0kl$ and $1kl$ reciprocal planes were recorded. Additionally, precession photographs were taken at 186 K. The reflection conditions found (hkl, $k + l = 2n$; $0kl$, k, $l = 2n$; $h00$, $h = 2n$) lead to the monoclinic non-conventional space group $A2_1/b11$ (or $A2_1/c11$). We choose space group $P2_1/n11$ for the primitive cell with the basic translations $t_1 = a$, $t_2 = (b + c)/2$, $t_3 = (-b + c)/2$. The basic vectors of the reciprocal lattice are then $t_1^* = a^*$, $t_2^* = b^* + c^*$, $t_3^* = -b^* + c^*$. For simplicity, the non-primitive setting will be used throughout this paper. The temperature-dependent lattice parameters calculated from a powder pattern on heating are represented in figure 5. Within the errors, the parameters a, b, c behave smoothly at $\zeta \rightarrow \varepsilon \rightarrow \delta$; only the monoclinic angle α seems to jump.

In a previous note (Jahn *et al* 1986), the non-primitive cell of ε-C_3CuCl was erroneously given as B centred. In fact, from a structural point of view the A centring is really unexpected. This can be seen from figure 6 where adjacent layers of the structure are projected onto the (001) plane at $z = 0$ and $\frac{1}{2}$, respectively. In the AF δ phase given in figure 6(a), the privileged short hydrogen bonds are directed almost along [100]; consequently, the tilt axes of chains and JT-distorted octahedra are nearly parallel to [010] (Doudin and Chapuis 1990a). We see that the long octahedron axes are uniformly aligned in (010) planes, and in the same planes octahedra and chains are tilted in antiphase ('AF state'). For the non-privileged hydrogen bonds we adopted the fully ordered scheme as has been reported for the analogous room-temperature phase of C_2CuCl (Tichy and Depmeier 1983). It is obvious that a F phase with an A-centred unit cell can be established only if the orientation of the octahedron axes is changed in a suitable way: in every second layer the in-plane octahedron axes have to exchange their lengths. In figure 6(b), this switching procedure has been performed for the octahedra at $z = \frac{1}{2}$. The arrangement obtained is compatible with the space group symmetries found. All short bonds retain their directions, in accordance with the smooth temperature behaviour of the lattice constants at the ε–δ transition and the very small birefringence difference between ε and δ. The non-privileged bonds can take the pattern drawn or an (010) mirror image of it. Our experimental results clearly support the existence of a reconstructive phase transition based on the change of the

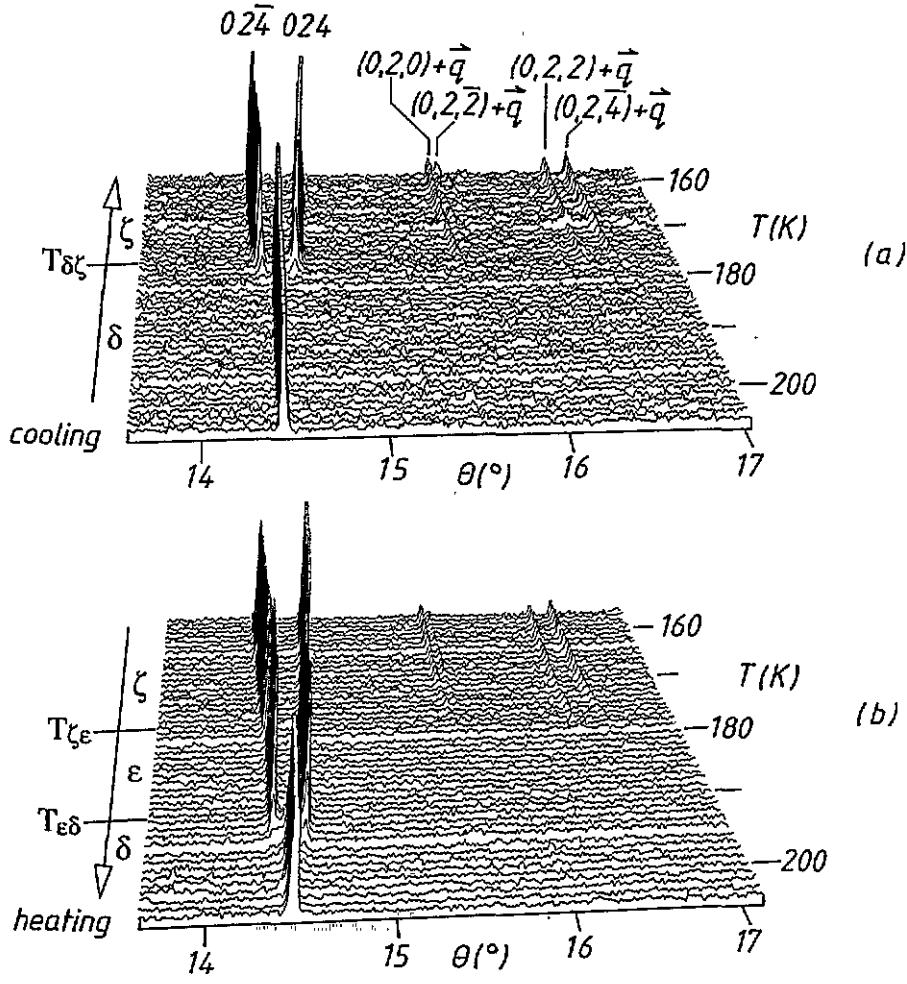

Figure 4. Variation in the main and the satellite reflections at the δ–ε–ζ transitions on (*a*) cooling and (*b*) heating. The reflections have been indexed with respect to the A-centred cell, as derived in section 3.3.

JT-distortion pattern. The process which switches between AF and F states may simply be termed 'octahedron-axes switching (OAS) in one layer'.

For the reconstructive phase transition discovered earlier in C_2CuCl (Jahn *et al* 1989), the structure switches between the space groups $Pbca$ (AF state) and $P2_1/n$ (F state); the non-primitive cell of $P2_1/n$ is B centred. The mechanism active at this transition is described best as 'hydrogen-bond switching' (HBS). The principle of this process can be seen by comparing figures 6(*b*) and 6(*c*); HBS rotates the hydrogen bonds by 90°, thus generating a fully new order and tilt pattern of chains and octahedra. It is important to note that the HBS and OAS active at the same transition would generate twin structures of the new phase. HBS is a more spectacular process than OAS; the lattice constants a and b exchange their lengths, and the birefringence $n_a - n_b$ changes sign. The domain phenomena due to these switching mechanisms will be discussed separately.

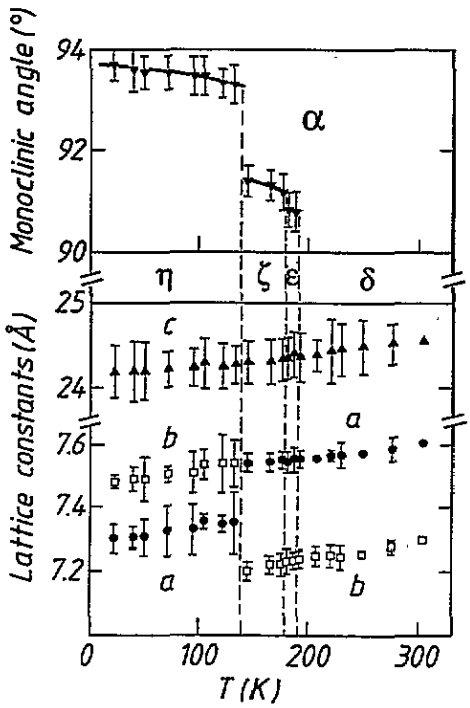

Figure 5. Lattice parameters of C_3CuCl as a function of temperature obtained by x-ray powder diffraction (on heating).

3.3. Low-temperature incommensurate ζ phase

Firstly rotating-crystal experiments at 140 K pointed to a cell doubling along b. The analysis of our high-resolution x-ray data shows, however, that the new reflections appearing below 180 K (figure 4) belong to a rather complicated modulation of the lattice having wavevector components along b^* and c^*. An experimental estimation of the c^* component from precession photographs failed; the resolution is poor because of the large c-value; additionally, twinning and the change in the direction of b^* due to monoclinic symmetry were cumbersome. We decided to attack the problem by a trial-and-error method. If the components of the modulation wavevector are approximated by rational numbers, then from the line positions of both main and satellite reflections the lattice parameters of the corresponding supercell can be calculated by a least-squares routine. The standard deviation between the measured and calculated diffraction angles $\delta\theta$ can be taken as an index for the goodness of the fit.

The part of the $0kl$ plane which has been studied by use of the focusing single-crystal camera is shown in figure 7. A centring and the glide plane rule out the points with $k + l = 2n + 1$ and $k = 2n + 1$. The full circles and crosses represent the observed main and satellite reflections, respectively; the location of the crosses anticipates the result of our treatment. The modulation vector $q = \kappa_1 a^* + \kappa_2 b^* + \kappa_3 c^*$ that we have to discuss starts from an allowed Bragg point; its range is given by $-\frac{1}{2} \leqslant \kappa_1, \kappa_2 \leqslant \frac{1}{2}$, $-1 \leqslant \kappa_3 \leqslant 1$. The x-ray results suggest that $\kappa_1 = 0$; a structure determination would have to decide whether there is a C component $\kappa_1 = 1$.

Least-squares fits were performed using the positions of eight main and 15 satellite reflections of the type $0kl$. The fitted parameters were the lattice constants b and c, the

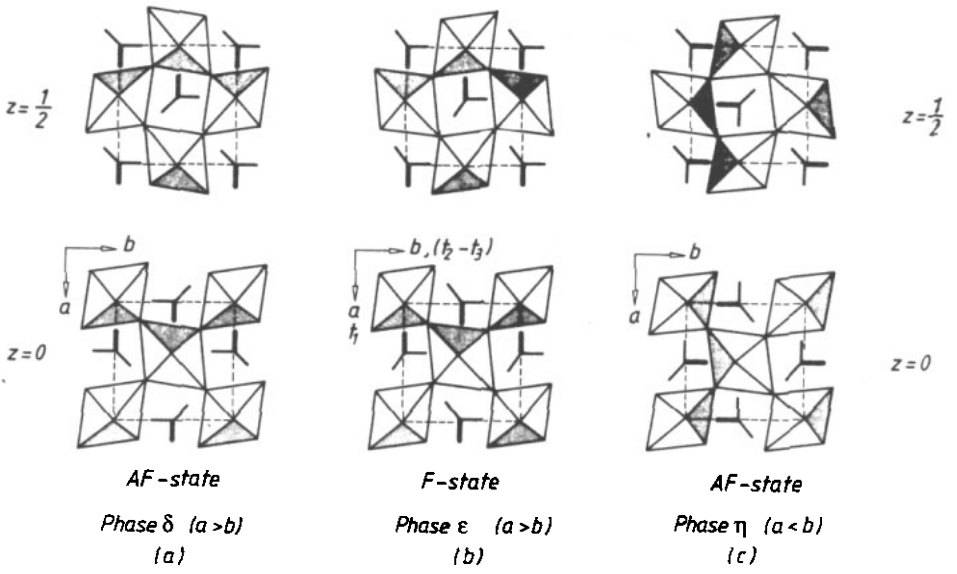

Figure 6. Schematic representtion of the structure of C_3CuCl in the c phases studied. Only elements characterizing the tilt or order patterns have been drawn. The octahedra indicate the JT distortion and the tilt pattern. Orientational order and tilts of the propyl-ammonium groups are represented by the hydrogen bonds (triangles); the shortest bonds have been marked. The groups above the projection plane and those below (not shown) are transformed into each other by a centre of inversion.

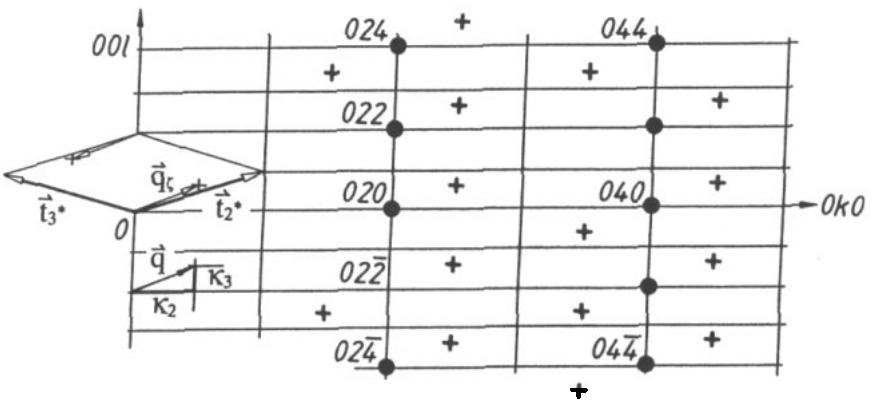

Figure 7. Main reflections and satellites of the ζ phase in the $0kl$ reciprocal plane of the face-centred unit cell; t_2^* and t_3^* are the reciprocal-lattice vectors of the primitive cell.

monoclinic angle α and an additive term correcting for an eventual zero-point offset of the diffraction angles. For a simple cell doubling ($\kappa_2 = \frac{1}{2}$; $\kappa_3 = 0$), no agreement exists between the measured and calculated line positions. If a modulation of $\kappa_2 = \frac{1}{2}$, $\kappa_3 = 1$, were correct, the 'splittings' of the satellite 'pairs' shown in figure 4 would have to be doubled. Help in finding a better κ_3 starting value came from the study of C_3CuBr running in parallel.

This compound shows a similar modulation. Incidentally, the 'splittings' of the satellite

reflections mentioned are nearly zero. In this case, the modulation component κ_3 could be calculated from the Bragg equation. With the lattice parameters determined from the main reflections, and assuming that $\kappa_2 = \frac{1}{2}$, we obtained $\kappa_3 \simeq 0.7$. Using this starting value for C_3CuCl, the modulation vector components κ_2 and κ_3 could be localized. Figure 8 presents the result for a measurement at 152 K; the standard deviations $\delta\theta$ of supercell fits obtained at several C points (crosses), were interpolated graphically in order to show the field of probable κ_2 and κ_3-values for $\delta\theta \leqslant 0.01$ and 0.02, respectively. At $\kappa_2 = 99/200$, $\kappa_3 = 11/17$, the minimum standard deviation $\delta\theta \simeq 0.008°$; a best fit with the eight main reflections alone yields $\delta\theta \simeq 0.004°$. The factor of 2 is mainly due to the uncertainty in determining the line position of the weak satellites.

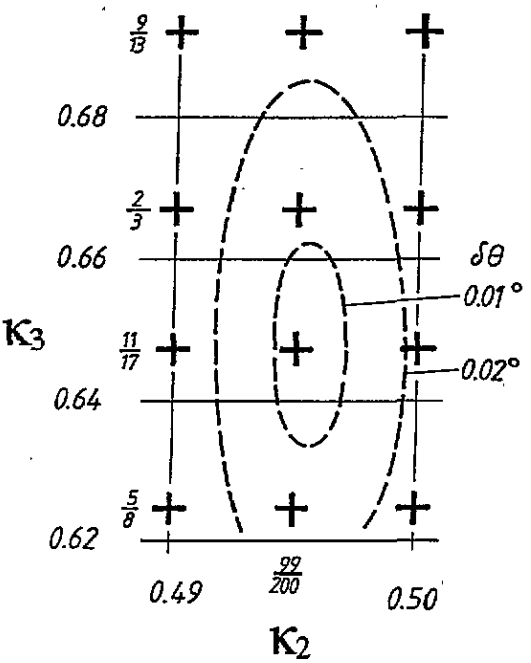

Figure 8. Determination of the modulation wavevector components κ_2 and κ_3 at 152 K (details in the text).

In order to check reproducibility and accuracy, the same procedure was performed for two data sets of another crystal, obtained at different cooling runs. The results given in figure 9 show that the modulation around 150 K can be represented by $q = (0.496 \pm 0.001)b^* + (0.654 \pm 0.005)c^*$. The corresponding modulation wavevector with respect to the primitive cell is $q_\zeta = (0.575 \pm 0.003)t_2^* + (0.079 \pm 0.002)t_3^*$. The temperature dependence of q was not studied in detail; the results for 170 and 130 K (figure 9) seem to indicate a variation along b^* of about 0.006 in this range. The effect of C_3MnCl is of the same order (Depmeier and Mason 1983); in C_3CdCl the temperature dependence was not resolvable within the error of $0.005b^*$ (Doudin and Chapuis 1988).

3.4. Reconstructive ζ–η phase transition

At the lock-in transition of C_3MnCl at 113 K, the birefringence decreases by about 5%; the thermal hysteresis amounts to 2 K (Brunskill and Depmeier 1982). For C_3CuCl, Etxebarria

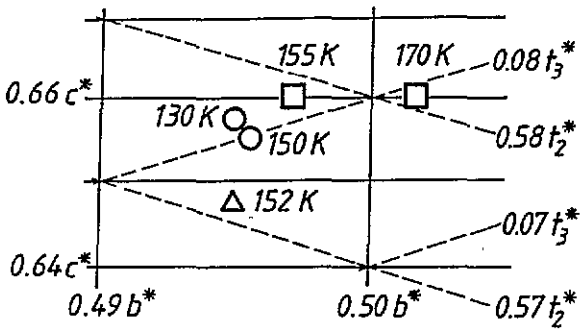

Figure 9. End point of the modulation vector at different temperatures, given for the face-centred cell (b^*, c^*) and the primitive cell (t_2^*, t_3^*), respectively, of the ζ phase. Identical symbols refer to the same cooling run.

et al (1988) report a similar birefringence drop at 132 K (on cooling), but a large hysteresis of 10 K. They compare their specific heat and thermal expansion data with results for C_3MnCl and postulate the existence of a lock-in transition for C_3CuCl, too.

The result of our birefringence measurement is quite different. The curve given in figure 1 and the curve obtained by Etxebarria *et al* do not scale at all at low temperatures. The most important point is that our birefringence jumps and changes sign at the first-order ζ–η transition. We think that the method used by Etxebarria *et al* for monitoring the birefringence fails in the case of large birefringence changes if these are not compensated. We verified by microscopic inspection of (001) plates that the indicatrix orientation rotates reversibly in the whole crystal by about 90° around the layer normal. In addition, precession photographs taken at 150 and 100 K showed unambiguously that the lattice constant ratio switches from $a/b > 1$ in the ζ phase to $a/b < 1$ in η. Therefore, a lock-in transition has to be ruled out.

The transition is well defined and extremely sharp in unstrained crystals. Powder diffraction patterns indicate an enormous sensitivity to strains; at 20 K both ζ and η phases coexist. The reflection conditions extracted from the various x-ray studies are as follows: $0kl$, $l = 2n$; $h00$, $h = 2n$. Only reflections with k, $l \neq 0$ are split. The structure of the η phase is monoclinic with space group $P2_1/c11$ and with four formula units per cell. The temperature-dependent lattice constants from powder diffraction, given in figure 5, impressively show the switching of the lengths of a and b.

Our results for the ζ–η transition of C_3CuCl point to a strong similarity with the HBS transition in C_2CuCl. If we apply the switching procedure to the (F) average structure of the IC ζ phase of C_3CuCl, we would get an (AF) orthorhombic structure with space group $Pcab$, possibly a twin structure of the δ phase with $Pbca$. What we find is a distorted version; the space group $P2_1/c11$ is a direct subgroup of $Pcab$. Figure 6(c) represents the structural configuration suggested for the η phase.

4. Free energy versus temperature diagram

The stability range of the IC ζ phase is bounded on both sides by reconstructive phase transitions and, consequently, ζ is not symmetry related to its neighbouring δ and η phases. Surprisingly, between the δ and η phases themselves a group–subgroup relation holds.

This symmetry relation on the one hand and the different order schemes on the other hand suggest an explanation of the unusual phase sequence on the basis of two free-energy curves in a thermodynamic potential versus temperature diagram which intersect twice. As shown in figure 10, the AF system is energetically favourable at higher and lower temperatures, corresponding to the δ and η phases, respectively, and the F system with the ε and ζ phases is stable in the range between. Temperature variation around the intersection points cannot switch the system instantaneously between AF and F states, since an energy activation barrier inhibiting the reconstructive transitions has to be overcome. Thermal hysteresis of a phase transition is a measure of the barrier heights.

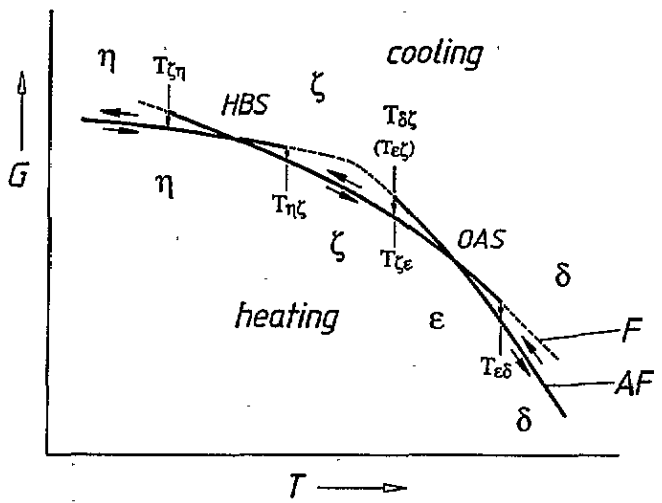

Figure 10. Schematic representation of the temperature-dependent free energy G of C_3CuCl in the structural phase sequence δ–ε–ζ–η. The full curves correspond to the possible states of the AF and F phases on cooling and heating, respectively.

The point of special interest is on the low-temperature side of the upper (OAS-driven) reconstructive transition. Our birefringence results (figure 1) show that the temperature $T_{\delta\zeta}$ of the irreversible $\delta \rightarrow \zeta$ transition coincides with the temperature $T_{\varepsilon\zeta}$ of the reversible hysteresis-free $\varepsilon \leftrightarrow \zeta$ transition. The question arises whether this is a fortuitous result or an indication that the OAS process is triggered by the IC lattice modulation. The other C_3MCl compounds studied so far favour low-temperature modulated phases with a modulation wave running parallel to the (b, c) plane, either along b as in the IC phases of C_3MnCl and C_3CdCl, or along $b \pm c$ as in the lock-in ζ phase of C_3MnCl. It is obvious that such a modulation could hardly develop in the δ phase of C_3CuCl; it would be hampered strongly by the alternating alignment of the octahedron axes in this plane (figure 6(a)). The experimental finding that the OAS transition on cooling is less influenced by strains than on heating also points to some kind of interaction between modulation and switching mechanism. Finally, the regular OAS process in every second layer of the crystal might even be controlled by the modulation component along c. The exciting phenomenon of the ε phase which arises only on heating is the consequence of both the trigger effect and the activation barrier of the OAS mechanism.

The AF state, favourable again at low temperatures, cannot be generated by a repetition of the OAS since the F alignment is stabilized by the lattice modulation. Instead of lowering

the energy by a lock-in transition as is the case in C_3CuBr (Schwab *et al* 1992), C_3CuCl prefers to undergo a second reconstructive phase transition using the HBS mechanism. The phase diagram of the mixed system $C_3CuBr_xCl_{1-x}$ is expected to show additional interesting features.

5. Conclusion

The structural phase sequence of C_3CuCl is unique within the large family of perovskite-type layer structures. C_3CuCl exhibits seven structural phases between 20 and 450 K, two of which are incommensurately modulated and, most surprisingly, two of the phase transitions at low temperatures are of the reconstructive type with no symmetry relation between subsequent phases. We succeeded in identifying these unusual structural phenomena by combining optical and x-ray measurements.

The degree of freedom responsible for the reconstructive phase transitions of the copper compounds is generated by the JT distortion of the $CuCl_6$ octahedra. The chain ordering is able to realize either a F or an AF phase. We find that the spontaneous switching between these configurations belongs to the standard repertoire of the copper compounds. Two mechanism are observed which, if active at the same transition, would lead to twin structures of the new phase; the OAS rotates the JT distortion of the octahedra in every second layer plane; the HBS induces a fundamental reorientation of chain and octahedron tiltings.

Basically, the very complex low-temperature sequence of C_3CuCl is caused by the incompatibility of the AF order scheme of the room-temperature δ phase with the modulation found generally in the C_3MX compounds. We therefore believe that the OAS δ–ζ transition is triggered by the IC modulation of the ζ phase. On heating, the large thermal hysteresis of the OAS transition allows the symmetrical ε phase to occur. At the low-temperature ζ–η transition, the F structure of C_3CuCl switches back to a distorted version of the AF room-temperature δ phase. As far as we know, C_3CuCl represents the only IC system in which a modulated phase is not symmetry related to its neighbouring phases of the sequence.

Acknowledgments

The authors wish to thank Professor W Prandl and Dr D Hohlwein for stimulating discussions, and Dr J Ihringer and A Endriss for advice on the x-ray powder method and microdensitometer handling. The crystals were grown by K Hagdorn-Wittern.

References

Arend H, Huber W, Mischgofsky F M and Richter van Leeuwen G K 1978 *J. Cryst. Growth* **43** 213
Brunskill I H and Depmeier W 1982 *Acta Crystallogr.* A **38** 132
Dachs H and Knorr K 1972 *J. Appl. Crystallogr.* **5** 338
Depmeier W 1983 *Solid State Commun.* **45** 1089
Depmeier W and Mason S A 1983 *Solid State Commun.* **46** 409
Doudin B and Chapuis G 1988 *Acta Crystallogr.* B **44** 495
—— 1990a *Acta Crystallogr.* B **46** 175
—— 1990b *Acta Crystallogr.* B **46** 180
Etxebarria J, Ruiz-Larrea I, Tello M Z and Lopez-Echarri A 1988 *J. Phys. C: Solid State Phys.* **21** 1717
Ihringer J 1982 *J. Appl. Crystallogr.* **15** 1
Jahn I R, Holocher K, Knorr K and Ihringer J 1986 *Z. Kristallogr.* **174** 102

Jahn I R, Knorr K and Ihringer J 1989 *J. Phys.: Condens. Matter* **1** 6005
Kind R 1980 *Ferroelectrics* **24** 81
Kusto W J 1988 *Ferroelectrics* **80** 285
Muralt P 1986 *J. Phys. C: Solid State Phys.* **19** 1689
Muralt P, Kind R, Blinc R and Zeks B 1982 *Phys. Rev. Lett.* **49** 1019
Muralt P, Kind R and Bührer W 1988 *Phys. Rev.* B **38** 666
Papst I, Fuess H and Bats J W 1987 *Acta Crystallogr.* C **43** 413
Saito K and Kobayashi J 1992 *Phys. Rev.* B **45** 10264
Schwab K, Jahn I R and Knorr K 1992 *Z. Kristallogr. Suppl.* **5** 231
Tichy K and Depmeier W 1983 *Würenlingen Report* AF-SSP-127 31